



Field study of a retaining wall constructed with clay-filled soilbags

Sihong Liu, Kewei Fan*, Siyuan Xu

College of Water Conservancy and Hydropower, Hohai University, Xikang Road 1#, Nanjing, 210098, China



ARTICLE INFO

Keywords:

Geosynthetics
Clayey soil
Field study
Retaining wall
Soilbags
Waterway project

ABSTRACT

This paper presents a field study of constructing retaining walls using soilbags that are formed by filling the excavated clayey soils into woven bags (geosynthetics). The strength and deformation of the soilbags filled with clayey soils were studied via laboratory tests. A 100 m testing retaining wall was constructed with soilbags in a waterway project. The lateral deformation, the lateral pressures and the surface settlements of the testing retaining wall were monitored during construction and after 7 months operation. The results show that the soilbags can increase the strength of clayey soils. After 7 months of the completion, the lateral deformation and the surface settlement of the testing retaining wall tend to be stable with the maximum values of 29.4 cm and 19.2 cm, respectively. The lateral earth pressure on the front retaining structure could be positively reduced owing to the interlayer's friction of soilbags. Compared to the conventional gravity concrete retaining wall, about 38% construction cost was saved in the 100 m testing retaining wall.

1. Introduction

Inland river navigation plays an important role in a modern comprehensive transportation system. The construction of high-grade waterways is required for the inland river navigation with the increase in quantities of shipments and large-scale freight ships. In plain areas, the construction of high-grade waterways usually produces massive clayey soils which should be treated properly. As the clayey soils have the characteristics of high water content, high compressibility and low strength (Wang and Luna, 2012; Naeini and Gholampoor, 2014; Butt et al., 2016; Jotisankasa and Rurgchaisri, 2018), they are usually treated as waste materials or backfilled behind walls after the dehydration or chemical improvement (Tremblay et al., 2002; Zhu et al., 2007; Quang and Chai, 2015; Dadouch et al., 2015). When the clayey soils are treated as waste materials, they not only occupy land resources, but also inevitably cause environmental pollution (Tang et al., 2001). The dehydration or chemical improvement of clayey soils is usually cost expensive and time consuming (Glendinning et al., 2007; Jeyakanthan et al., 2011; Shi et al., 2017). On the other hand, retaining walls, most commonly concrete/masonry gravity retaining walls, are usually constructed along the two banks of the approach channels in a waterway project. As gravity retaining walls require high bearing capacity of foundation, the soft foundation has to be treated, leading to relatively high cost of the project (Dong et al., 2004; Sadrekarimi and Abbasnejad, 2010). The alternative way to solve this problem is to use geosynthetic-reinforced earth retaining walls as they are weight light

and easily adapt to foundation deformation (Yang et al., 2009; Santos et al., 2014; Yoo, 2017; Song et al., 2018). Some geosynthetic-reinforced earth retaining walls constructed on soft foundations and the related researches have been reported (Rowe and Skinner, 2001; Skinner and Rowe, 2005; Huang and Luo, 2010; Santos et al., 2013; Xue et al., 2014; Zou et al., 2016).

As a result of extensive studies on soilbags, Matsuoka and Liu (2005) proposed a way of constructing retaining walls using soilbags, which could be regarded as a new type of the geosynthetic-reinforced earth retaining wall. Liu et al. (2014) investigated the distribution of the earth pressures behind a soilbags-stacked retaining wall and the lateral transmission in the retaining wall through laboratory experiments. The stability of soilbags-constructed retaining walls is closely related to the interlayer friction of soilbags, which is influenced by the bag friction, the grain sizes of filling materials and the interlayer arrangements of soilbags (Liu et al., 2016). The shaking table tests indicate that the soilbags-constructed retaining walls have a good seismic performance owing to the relatively flexibility of soilbags (Liu et al., 2015; Li et al., 2015). A primary design method for soilbags-constructed retaining walls has been proposed by Liu (2017). Several application cases and the well performance of this new type wall have been reported (Matsuoka and Liu, 2005; Liu, 2017). It has been found the soilbags-constructed retaining wall has the advantages of weight light and good adaptation to foundation deformation like the geosynthetic-reinforced earth retaining wall. However, it is noted that the infill materials of soilbags and the backfill materials of retaining walls in the past

* Corresponding author.

E-mail addresses: sihongliu@hhu.edu.cn (S. Liu), kw_fan@hhu.edu.cn (K. Fan), syxu@hhu.edu.cn (S. Xu).

application cases are mainly coarse granular materials or low-cohesion soils like sands, gravels and loamy soils, and clayey soils are seldom used.

This paper presents a case study of constructing a retaining wall using soilbags, in which the infill materials of soilbags and the backfill materials of the retaining wall are clayey soils excavated in a waterway project. The unconfined compression tests were carried out to investigate the strength and deformation properties of soilbags with the infill materials of clayey soils. The construction way of the clay-filled soilbags was proposed. The lateral deformation, the lateral pressures and the surface settlements of the retaining wall were monitored during the construction and after the completion for 7 months.

2. Properties of clay-filled soilbags

The strength and deformation properties of the soilbags filled with clayey soils were investigated through unconfined compression tests. The polypropylene-made bags with a mass weight of 150 g per-square meter were used. The tensile strengths of the bags are 37.1 kN/m and 28.0 kN/m in warp and weft directions, respectively. The warp and weft elongation are both less than 25%. The infill materials of the soilbags are the clayey soils, which were excavated in the field with the physical and mechanical properties as listed in Table 1.

The unconfined compression tests were carried out on three clay-filled soilbags that were stacked vertically, as shown in Fig. 1(a). One soilbag has a length of 66 cm, a width of 50 cm and a height of 7 cm. The device used was the same as the one for testing compressive strengths of concrete blocks. The vertical load was continuously applied on the stacked soilbags by uplifting the baseplate of the device at a speed of 3.5 mm/min until the breakage of soilbags happened, accompanying with the sudden decrease of the vertical load. The tests were repeated twice for the reproducibility. As shown in Fig. 1(a), it was obviously observed that there was water seeping from the bags during the compression, indicating that the woven bags have the capacity of filtering water and keeping infill soils. The soilbags became flatter after the tests with a dimension of about 73.2 cm × 54.5 cm × 5.4 cm. Fig. 1(b) shows the soilbag locally torn up in the warp direction in the middle of the top surface. Tantonio and Bauer (2008) numerically simulated a soilbag under vertical compression and found that the distribution of the tensile stress in the bag material in the circumference of the soilbag is not uniform in the case of the interlocked interface and the limit tensile stress is first reached at the middle part of the soilbag. This is in agreement with the experimental phenomena of Fig. 1(b). Fig. 2 gives the evolutions of the vertical loads with vertical compressive deformation of the two unconfined compression tests. The ultimate vertical loads of the soilbags are 560 kN and 620 kN, respectively, corresponding to the compressive strengths of 1.40 MPa and 1.55 MPa.

After the unconfined compression tests, the water content of the clayey soils inside the bags was measured to be 46.5% on average, which was lower than the initial one (before the compression tests) by 3.9%. Meanwhile, the shear strength of the infill clayey soils was measured by direct shear tests under the unconsolidated-undrained (UU) condition. Fig. 3 gives the measured shear strengths of the clayey soils in the three soilbags (averaging after the two compression tests). The strength parameters of the infill clayey soils are: $c = 15.4$ kPa, $\phi = 10.8^\circ$. Compared to the initial ones, the cohesion of the infill clayey soils changes slightly, but the internal friction angle increases by 4.9° owing to the enhancement of the inter-particle contacts of the infill clayey soils.

Theoretically, the unconfined compressive strength σ_v of soilbags (Matsuoka and Liu, 2005) can be predicted by

$$\sigma_v = \frac{2T}{B} \left(\frac{B}{H} \cdot K_p - 1 \right) + 2c \sqrt{K_p} \tag{1}$$

where B and H are the width and the height of the soilbag, respectively;

Table 1
Physical and mechanical properties of the clayey soils.

Water content (%)	Dry density (g/cm ³)	Void ratio	Liquid limit	Plastic limit	Consolidation coefficient (10 ⁻⁴ cm ² /s)	Compression coefficient (MPa ⁻¹)	Permeability coefficient (10 ⁻⁷ cm/s)	Cohesion (kPa)	Inter-frictional angle (°)
50.4	1.16	1.42	40.3	22.3	3.08	1.34	4.25	16.0	5.9



Fig. 1. Unconfined compression tests on clay-filled soilbags: (a) Schematic view; (b) Under compression; (c) Torn place on the soilbag surface.

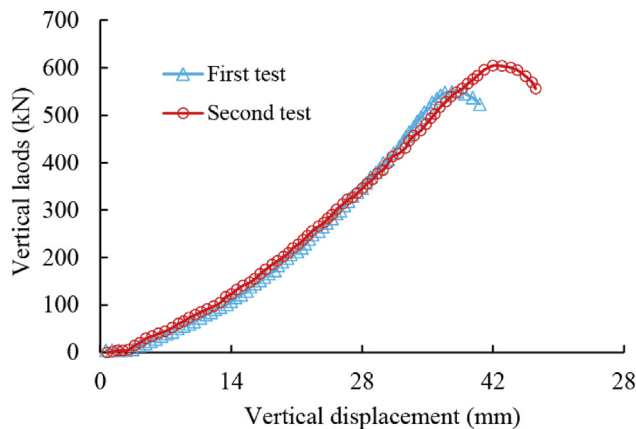


Fig. 2. Results of unconfined compression tests on soilbags.

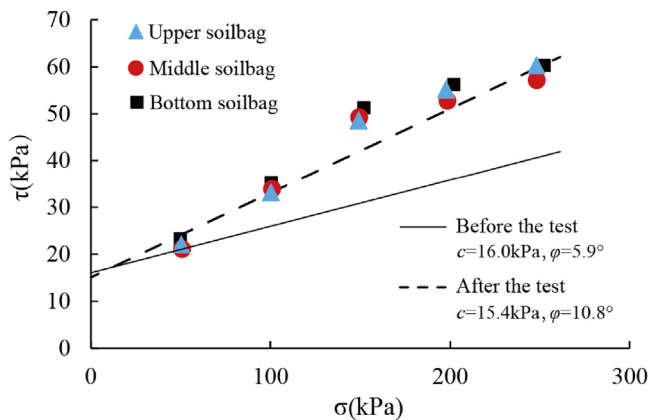


Fig. 3. Shear strength of the infill soils before and after the compression tests.

T is the tensile strength along the bag. K_p is equal to $(1 + \sin\varphi)/(1 - \sin\varphi)$; c and φ are the cohesion and the internal friction angle of the infill soils, respectively. By using the tensile strength T of 37.1 kN/m in the warp direction, the compressive strength σ_v of the soilbags tested is calculated to be 1.45 MPa, which agrees well with the measured values. As the compressive strength of 1.45 MPa is equivalent to the 1/10 compressive strength of C25 concrete, the soilbag filled with the clayey soils may be regarded as a “soft rock”. The high compressive strength of the soilbags is attributed to the tensile force of the bag that enhances the contacts between the soil particles inside the bag, resulting from the extension of the bags perimeter under the action of external loads.

In conclusion, if the clayey soils are filled into a woven bag to form a soilbag, it has a high compressive strength and thus can be used to construct retaining walls.

3. Testing retaining wall with soilbags

3.1. Design of the retaining wall

A 100 m long testing retaining wall with a height of 5 m was built on a soft foundation in the navigation channel of a waterway project. The soft foundation mainly consists of three layers (see Fig. 4): the first layer of artificially backfilled soil near the ground surface (EL. 2.20 m) with an average thickness of 1.2 m, the second layer of clayey soils approximately located between EL.1.00 m and EL.-19.00 m, and the third layer of silt clays below EL.-19.0 m. The first layer was excavated and abandoned in the project. The clayey soils excavated in the second layer were directly filled into the woven bags to form soilbags, which were used to build the retaining wall. The properties of the clayey soils have been given in Table 1.

Fig. 4 shows the design of the retaining wall constructed with clay-filled soilbags. A 0.6 m thick and 5 m high L-type concrete facing was designed to protect the collision of passing ships on the retaining wall, which was built using C25 concrete (the compressive strength is 25 N/mm²) on the foundation treated with cement mixing piles. And a 0.5 m thick concrete ribbed slab is installed behind the L-type wall with an interval of 3.5 m. Behind the L-type concrete facing, the clay-filled soilbags were backfilled, which were arranged in a staggered form. The soilbags have two sizes: one is 120 cm × 120 cm × 30 cm and the other is 120 cm × 60 cm × 30 cm. Apart from the bottom, the width of the soilbags retaining wall is 3.6 m, three columns of 120 cm × 120 cm × 30 cm soilbags. The excavation slope of the navigation channel was designed to be 1:4 on the basis of the stability calculation. On the excavation slope, three columns of 120 cm × 120 cm × 30 cm soilbags were placed. Between the soilbags behind the L-type concrete facing and those on the excavated slope, the clayey soils were directly backfilled. Every 30 cm high the backfilled soil was patted using the excavator bucket for 4 times. Every four layers of the soilbags were wrapped with HDPE uniaxial geogrids that has an ultimate tensile strength of 65 kN/m, a tensile strength of 31 kN/m at 5% strain and an ultimate tensile strain of 12%.

3.2. Construction of clay-filled soilbags

Usually, soilbags are made in advance on some places near the construction site and then transported to the construction site to be laid. However, in the case that clayey soils are used as the infilled materials of soilbags, this construction way is not applicable as clayey soils excavated in fields are high sticky and cake-like and hard to be filled into woven bags. For this reason, we designed a kind of box-shaped bags and proposed an in-place construction method. The box-shaped bag was made of polypropylene with a weight of 150 g per-square meter, as used in the laboratory tests. The opening of the bag is positioned on the top surface, where clayey soils can be filled in by excavators, as shown in the Fig. 5 (a). An iron frame that can contain simultaneously three bags was also designed, as shown in Fig. 5 (b). Instead of the traditional construction method, the proposed in-place construction method is to fill clayey soils into bags in the construction site and move the iron

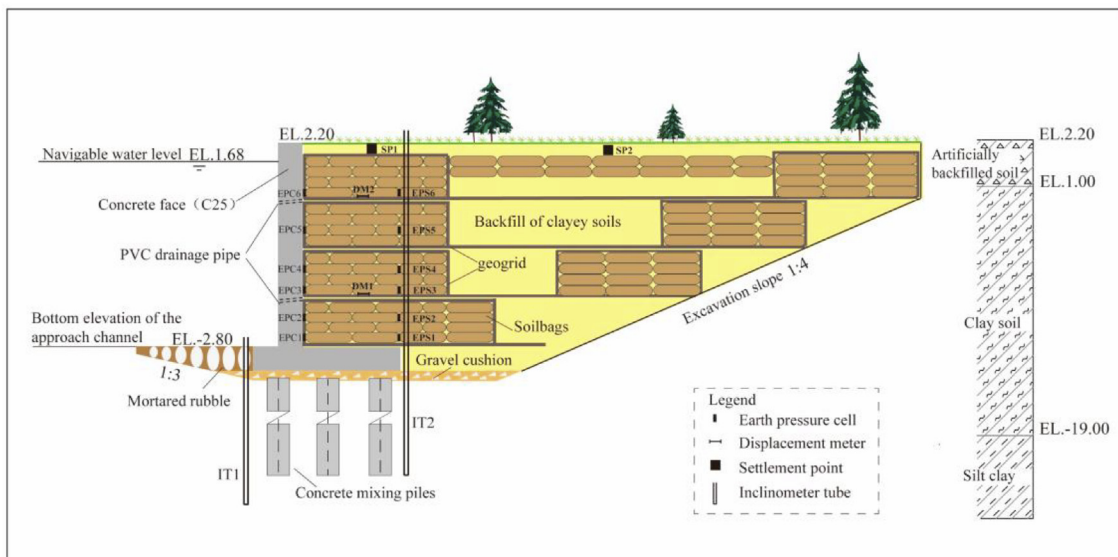


Fig. 4. Schematic view of the retaining wall constructed with soilbags.

frame to the next place after the sealing of the soilbags, as shown in Fig. 5 (c) and (d). A hand sewing machine and nylon threads were used to sew soilbags. The nylon thread has a tensile strength of about 700 kN/m, much greater than the tensile strength of the woven bags. The opening on the top surface of the boxed bag has four sides. The inner two short sides were firstly sewed and the outside two long sides were then sewed.

Fig. 6 shows the proposed in-place construction method applied in the testing retaining wall. The construction process is as follows: 1) three box-shaped bags were placed into the frame and the clayey soils were filled into the bags using a backhoe (Fig. 6(a)); 2) after the sealing of the bags with a hand sewing machine, the frame was lifted with the backhoe and moved to the next place adjacent to the filled soilbags (Fig. 6(b)); 3) the filled soilbags were compacted with the backhoe to ensure the development of the bag tensile force and to reduce the settlement of the retaining wall after the completion. The interstices between the completed soilbags as shown in Fig. 6(c) would be filled with the infill soils of the bags; (4) when four layers of the soilbags behind

the L-type concrete facing and those on the excavated slope were completed, they were wrapped with HDPE uniaxial geogrids, as shown in Fig. 6(d). Thirty soilbags could be constructed per hour in this testing retaining wall.

3.3. Monitoring instruments

In order to evaluate the behavior of the testing retaining wall, a number of monitoring instruments were installed in the middle section of the testing retaining wall during the construction. As shown in Fig. 4, the instruments include twelve earth pressure cells (denoted as EPC1-6 and EPS1-6), two inclinometer tubes (IT1 and IT2 in front of the L-type concrete facing and IT2 in the retaining wall of soilbags), two displacement meters on the geogrids (DM1 and DM2) and two settlement observation points on the top surface of the retaining wall (SP1 and SP2, 1.8 m and 12.5 m away from the L-type concrete wall, respectively).

The 10 m long retaining wall with the instruments installed were constructed from January 26th to 29th, 2015, which was regarded as

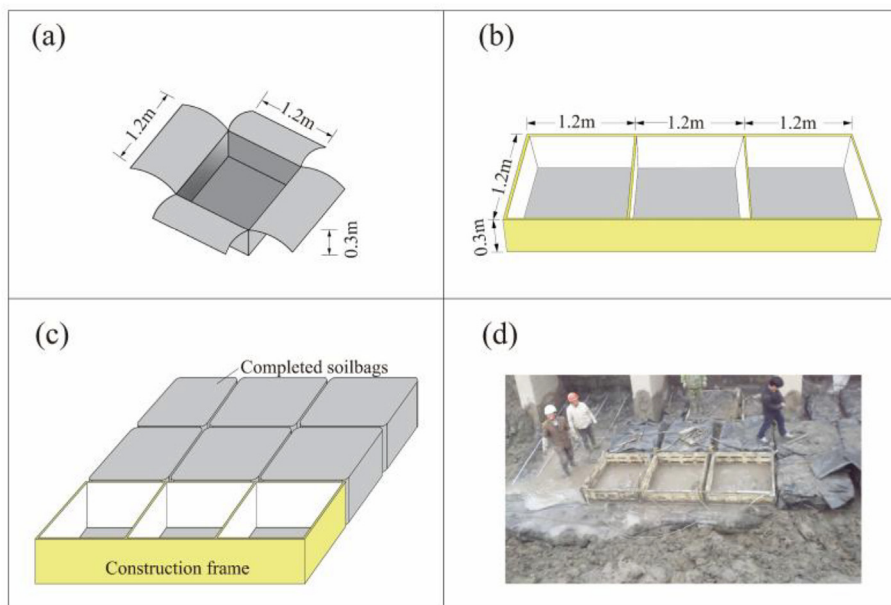


Fig. 5. In-place construction method of soilbags filled with clayey soils: (a) Box-shaped bag; (b) Construction frame; (c) Schematic view; (d) Field photo.

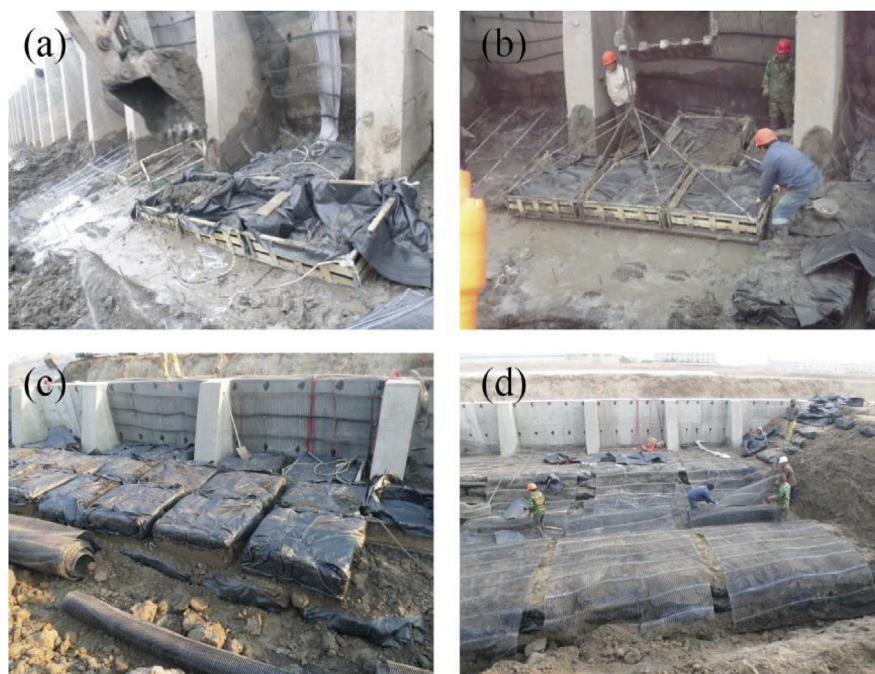


Fig. 6. In-place construction of soilbags for the testing retaining wall; (a) Filling clayey soils into bags; (b) Moving the frame; (c) Completed soilbags; (d) Wrapping geogrids.

the construction period in the monitoring period. During the construction period, the earth pressures behind the L-type concrete facing and in the retaining wall of soilbags and the displacements of the geogrids as well as the lateral displacements in front of the L-type concrete facing were measured. After the completion of the retaining wall, the IT2 inclinometer tube and the two settlement observation points of SP1 and SP2 were monitored in addition to the measurements during the construction period. The waterway was open to navigation in June 4, 2015. In the monitoring, the period from 2015 to 02-01 to 2015-06-03 and the period after 2015-06-04 were called as the completion period and the operation period, respectively. The monitoring was stopped at 2015-08, as the measured earth pressures and the displacements were basically unchanged.

4. Monitored results

4.1. Lateral displacements

Fig. 7 shows the lateral displacements of the foundation and the retaining wall of soilbags measured by the inclinometer tubes IT1 and IT2. It can be seen from Fig. 7(a) that the lateral displacement of the foundation in front of the L-type concrete facing (IT1) increases during the construction of the soilbags and develops further after the completion of the soilbags. The maximum measurement of IT1, occurring on EL.-4.0 m of the gravel cushion, is 10.0 mm at the end of construction (2015-01-29) and reaches 19.2 mm at 2015-06-03, i.e. the increment is 9.2 mm during the completion period. When the waterway was open to navigation at 2015-06-04, the inclinometer tube IT1 was submerged and the measurement was stopped. The inclinometer tube IT2 began to be measured at the end of construction (2015-02-01). Fig. 7(b) shows the evolution of the lateral displacement of the retaining wall of soilbags and the foundation measured by IT2. During the completion period, the maximum lateral displacement of the retaining wall of soilbags is 29.4 mm, occurring at the top surface. The lateral displacement on EL.-4.0 m of the gravel cushion measured by IT2 at 2015-06-03 is 9.92 mm, which is very close to the measurement of IT1 on EL.-4.0 m. At the start of the operation of the waterway, the measurement of IT2 turns to be decreased owing to the action of water pressure. At 2015-07-

15, the maximum value at the top surface was measured to be 22.5 mm, which was basically unchanged at 2015-08-15. Fig. 7(c) shows the distribution of the lateral displacements of the retaining wall of soilbags relative to the foundation. It can be seen that the retaining wall of soilbags deforms laterally like a cantilever with a maximum lateral displacement of 21.2 mm at the top surface before the waterway operation and a relatively unchanged value of 16.6 mm after the operation. The ratio of the lateral deformation to the height of the retaining wall is about 0.42%, less than 1.0% of the geo-synthetics retaining wall reported by Zhang and Han (2012).

4.2. Lateral earth pressures

Fig. 8 shows the evolution of the lateral earth pressures behind the L-type concrete facing and within the soilbags during the construction, measured by EPC and EPS, respectively. As expected, they increase with the increase in the height of the soilbags retaining wall. As a result of the interlayer friction of soilbags, the values of EPC measurement are smaller than those of EPS measurement. Fig. 9 shows the distributions of the lateral earth pressures behind the L-type concrete facing and within the soilbags along the height of the wall at the end of the construction. They are close to the distributions of the static and the active earth pressures, respectively. As the interlayer friction of soilbags increases with the increase in the applied upper stress (Liu et al., 2016), the difference between the EPC measurement and the EPS measurement increases gradually from the top to the bottom of the retaining wall, except for the lowest EPC1 and EPS1 owing to the bottom constraint.

4.3. Top surface settlements

Fig. 10 shows the evolution of the top surface settlements of the retaining wall after the completion of the retaining wall of soilbags measured at the points of SP1 and SP2. As shown in Fig. 4, the point SP1 is located on the top surface of the retaining wall of soilbags and the point SP2 is on the top surface behind the retaining wall alternately backfilled with soilbags and clayey soils. It can be seen from Fig. 11 that the top surface settlement measured at the point SP1 is larger than that measured at the point SP2 at the initial stage after the completion of the

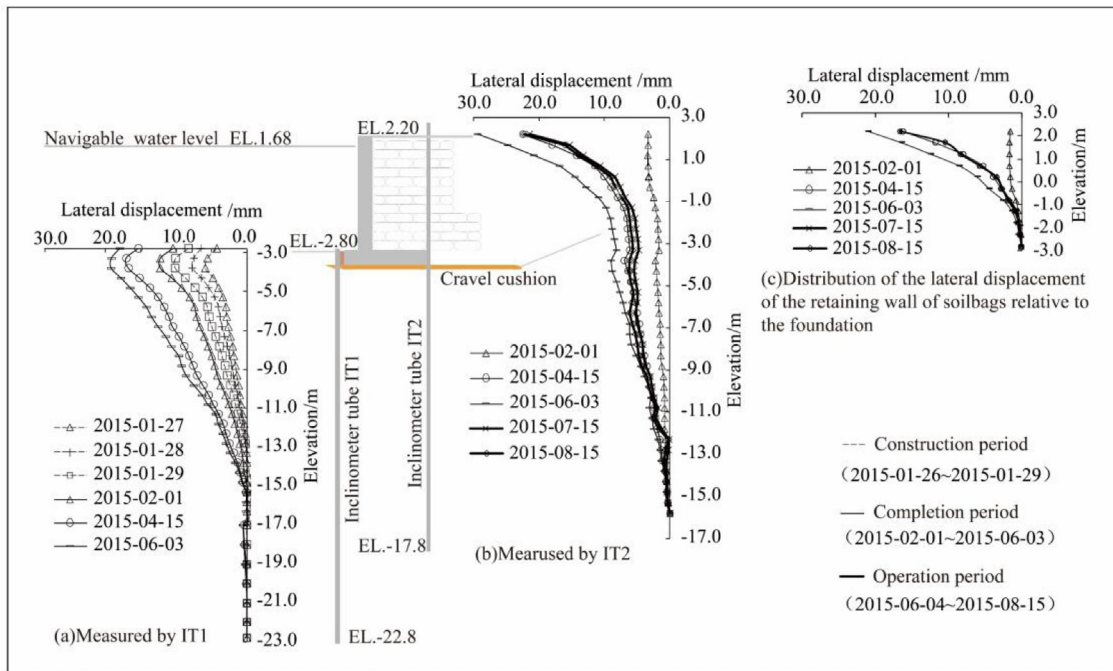


Fig. 7. Measured results of the inclinometer tubes IT1 and IT2.

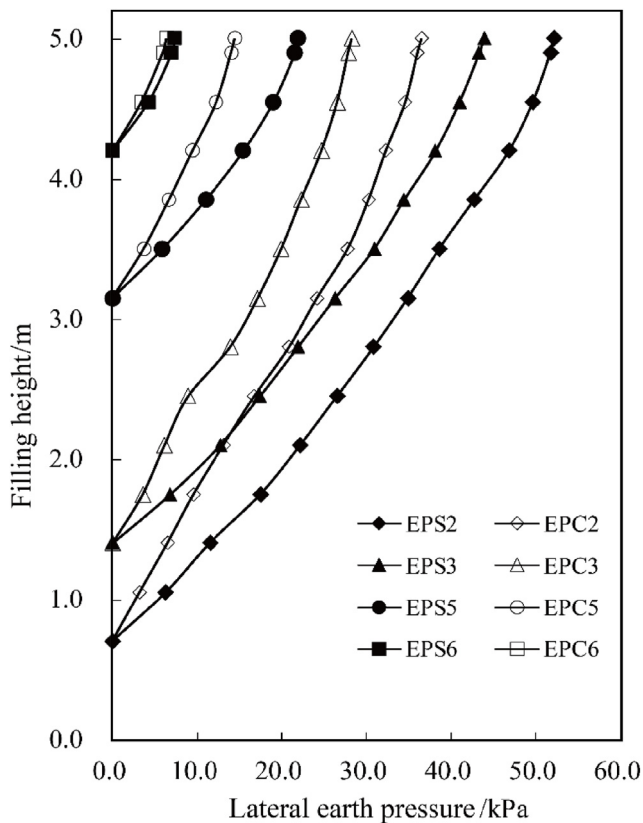


Fig. 8. Evolution of the lateral earth pressures behind the concrete facing and in the soilbags during construction.

construction (from 2015 to 02-01 to 2015-04-15) because the soilbags retaining wall has a free drainage boundary and consolidates faster than its backfill. During the period of 2015-4-15 to 2015-5-15, the settlement measured at point SP2 increased significantly, likely resulting from the passage of construction machinery. After 7 months of the completion

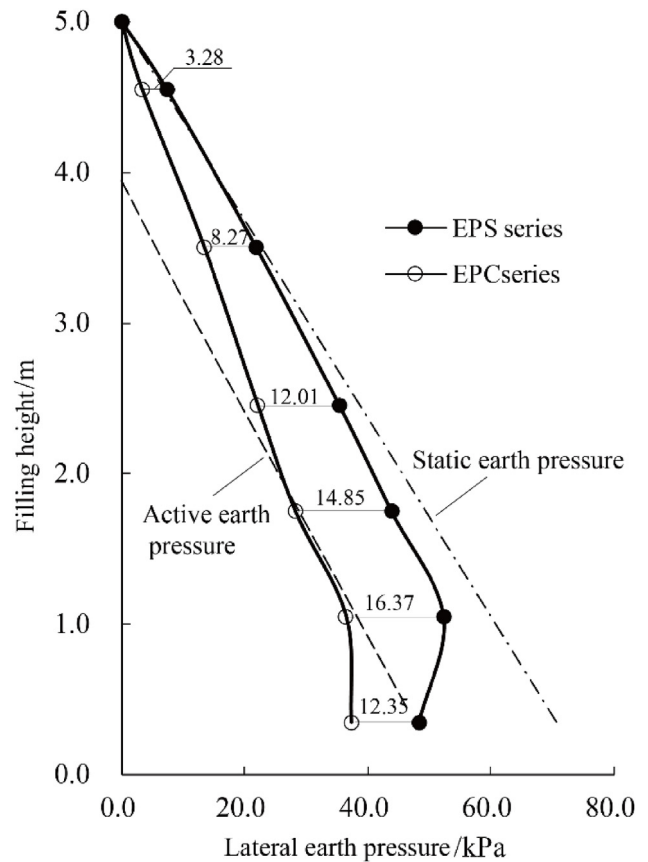


Fig. 9. Distribution of the lateral earth pressures behind the concrete facing and in the soilbags along the wall height at the end of construction.

(2015-08-15), the settlements measured at the points SP1 and SP2 are 19.2 cm and 22.8 cm, respectively. After 3 months of the completion, the rate of settlements at the points SP1 and SP2 is less than 2 mm per month from 2015 to 04-15 to 2015-08-15. The top surface settlement

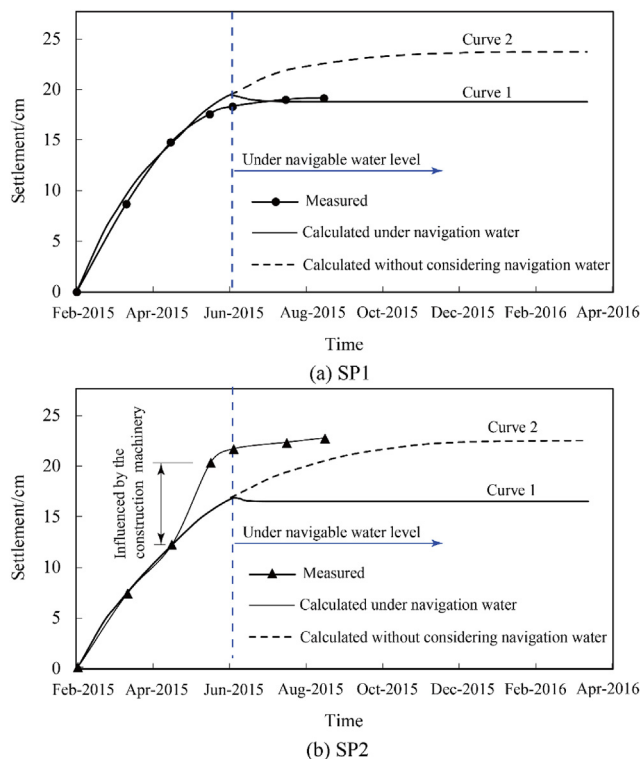


Fig. 10. Top surface settlement-time relationships of the retaining wall after the completion.

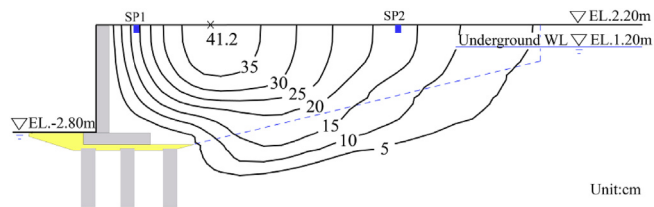


Fig. 11. Contours of the settlement in the retaining wall at 2015-06-03.

and the horizontal displacement of the retaining wall (see Fig. 8) illustrate that the deformation of the retaining wall has tended to be stable after 7 months.

The settlement of the retaining wall is closely related to the consolidation of the clayey soils inside the soilbags, which was analyzed by using the finite element method. The modified Cam-clay model was used to simulate the mechanical behavior of the clayey soils. The model parameters of the clayey soils were estimated from the experimental results given in Table 1. The reinforcement of soilbags was considered by introducing an apparent cohesion c_T due to the bag tension (Matsuoka and Liu, 2005; Liu et al., 2018). The apparent cohesion c_T and the permeability k of the assembly of the soilbags were estimated to be 30 kPa and 6.4×10^{-7} cm/s, respectively, through the finite element back analysis (Hird et al., 1992; Likar and Vukadin, 2003; Chai et al., 2014) by using the field monitored settlements at the points SP1 and SP2. The permeability of the assembly of the soilbags obtained from the back analysis is about 1.5 times that of the clayey soils. That the permeability of the soilbags assembly is not greatly increased is because the gaps among the soilbags are filled with clayey soils. The calculated settlement-time relationships at the points SP1 and SP2 are also given in Fig. 10, in which curves 1 and 2 represent respectively the calculation results considering and not considering the action of the navigation water on the retaining wall. It is understood that under the action of the navigation water, the retaining wall of soilbags is slightly compressed with a little decrease of the settlements of the top surface. As

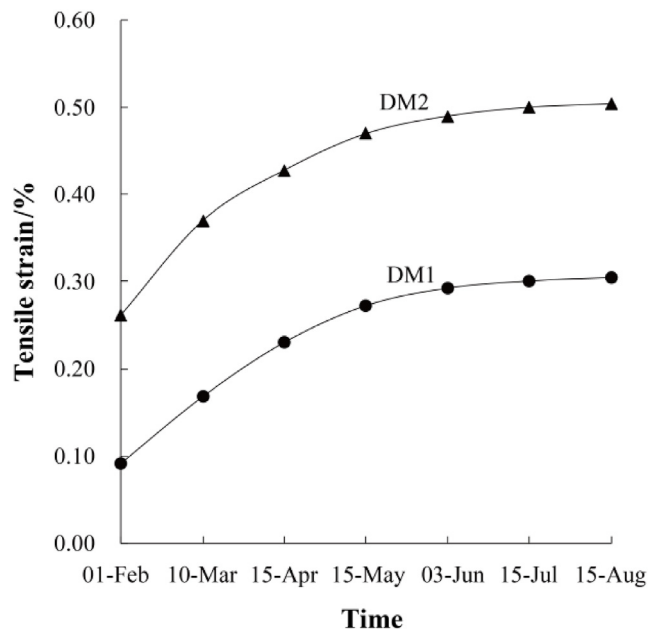


Fig. 12. Evolution of the tensile strains in the geogrids after the completion of the construction.

mentioned, the passage of construction machinery caused the significant increase of the settlement at point SP2 from 2015-4-15 to 2015-5-15. This is why the great difference exists between the calculation and the measurement at point SP2 after 2015-4-15. After impounding in the navigation channel, the pore water pressure within the retaining wall of soilbags increase slightly, which is unfavorable to the consolidation of the clayey soils inside the soilbags. Here, the average degree of consolidation of the clayey soils inside the soilbags retaining wall before the impounding (2016-06-03) is estimated from the curve 2. The final settlements at point SP1 is predicted to be 23.7 cm from curve 2, corresponding to the consolidation degree of 83.5%. Fig. 11 shows the contours of the calculated settlement of the retaining wall at 2015-06-03. The maximum settlement is 41.2 cm, appearing in about 2 m horizontally behind the wall.

4.4. Tensile strains of the wrapping geogrids

Fig. 12 shows the evolution of tensile strains of the wrapping geogrids after the completion of the construction. Both the tensile strains measured by FC1 and FC2 increase at the first three months after the completion of the construction, and then tend to be unchanged. In accordance with the decreasing lateral displacement of the retaining wall along the height from the top to the bottom, the tensile strain measured by FC2 is larger than that by FC1. After 7 months of the completion of the construction (2015-05-15), the tensile strains of the wrapping geogrids were measured to be 0.304% and 0.504% by FC1 and FC2, respectively, corresponding to the tensile strengths of 2.432 kN/m and 5.248 kN/m (far less than the geogrid ultimate tensile strength of 69.17 kN/m). This measurement suggests that the high tensile strength of the wrapping geogrids may not be needed in such projects.

By the way, the overall construction cost of this 100 m long testing retaining wall was estimated to be 62% of the concrete gravity retaining wall as constructed in the same waterway project.

5. Conclusion

The unconfined compression tests were carried out on the soilbags filled with clayey soils in laboratory and a testing retaining wall was constructed with the clay-filled soilbags in the field of a waterway project and monitored during the construction and after the completion

for 7 months. Based on the laboratory tests and field monitored results, the following conclusions can be obtained:

- (1) Clayey soils can be used to construct retaining walls if they are filled into woven bags to form soilbags. The soilbags filled with clayey soils have high compressive strengths resulting from the tensile forces of woven bags.
- (2) The designed box-shaped bags and the proposed in-place construction method are applicable for soilbags filled with clayey soils and the high efficiency of the construction has been proved in the testing retaining wall.
- (3) The field monitoring data indicates that the retaining wall constructed with the soilbags filled with clayey soils performs well. The maximum lateral displacement and the surface settlement of the testing retaining wall are 29.42 cm and 19.2 cm, respectively, which tend to be unchanged after the completion of the construction for 7 months. The lateral earth pressure on the front concrete facing is positively reduced owing to the interlayer's friction of soilbags.
- (4) The cost of the retaining wall constructed with soilbags can be greatly reduced compared to the gravity concrete retaining wall. The overall construction cost of the 100 m long testing retaining wall was estimated to be 62% of the concrete gravity retaining wall as constructed in the same waterway project.

Acknowledgments

This work was supported by the National Natural Science Foundation of China (Grant No. 51379066). It was also a part of work in the project funded by the Priority Academic Program Development of Jiangsu Higher Education Institutions (PAPD), China (Grant No. YS11001). These supports are gratefully acknowledged.

References

- Butt, W.A., Mir, B.A., Jha, J.N., 2016. Strength behavior of clayey soil reinforced with human hair as a natural fibre. *Geotech. Geol. Eng.* 34, 411–417.
- Chai, J.C., Horpibulsuk, S., Shen, S.L., Carter, J.P., 2014. Consolidation analysis of clayey deposits under vacuum pressure with horizontal drains. *Geotext. Geomembranes* 42, 437–444.
- Dadouch, M., Ghembaza, M.S., Ikhlef, N.S., 2015. Study in laboratory of treatment with cement of silty material: improvement of the mechanical properties. *Arab. J. Geosci.* 8, 4329–4336.
- Dong, P., Qin, R., Chen, Z., 2004. Bearing capacity and settlement of concrete-cored DCM pile in soft ground. *Geotech. Geol. Eng.* 22, 105–119.
- Glendinning, S., Lamont-Black, J., Jones, C.J.F.P., 2007. Treatment of sewage sludge using electrokinetic geosynthetics. *J. Hazard Mater.* 139, 491–499.
- Hird, C.C., Pyrah, I.C., Russell, D., 1992. Finite element modelling of vertical drains beneath embankments on soft ground. *Geotechnique* 3, 499–511.
- Huang, C.C., Luo, W.M., 2010. Behavior of cantilever and geosynthetic-reinforced walls on deformable foundations. *Geotext. Geomembranes* 28, 448–459.
- Jeyakanthan, V., Gnanendran, C.T., Lo, S.C.R., 2011. Laboratory assessment of electro-osmotic stabilization of soft clay. *Can. Geotech. J.* 48, 1788–1802.
- Jotisankasa, A., Rurgchaisri, N., 2018. Shear strength of interfaces between unsaturated soils and composite geotextile with polyester yarn reinforcement. *Geotext. Geomembranes* 46, 338–353.
- Li, L.J., Liu, S.H., Xu, X.D., Zhang, Y.Z., Li, D., 2015. Experimental study of effects of soil fills on dynamic characteristics parameters of soil-bags. *Rock Soil Mech.* 36, 131–138 (in Chinese).
- Likar, J., Vukadin, V., 2003. Time-dependent back analysis of a multianchored pile retaining wall. *J. Geotech. Geoenviron. Eng.* 129, 91–95.
- Liu, S.H., Li, L.J., Zhang, Y.Z., Xu, X.D., Xue, X.H., 2015. Small-scale shaking table tests on retaining wall constructed with soilbags. *J. Hohai Univ.* 43, 237–243 (in Chinese).
- Liu, S.H., 2017. Principle and Application of Soilbags. Science Press, Nanjing (in Chinese).
- Liu, S.H., Fan, K.W., Chen, X.L., Jia, F., Mao, H.Y., Lin, Y.W., 2016. Experimental studies on interface friction characteristics of soilbags. *Yantu Gongcheng Xuebao/Chinese J. Geotech. Eng.* 38, 1874–1880 (in Chinese).
- Liu, S.H., Jia, F., Shen, C.M., Weng, L.P., 2018. Strength characteristics of soilbags under inclined loads. *Geotext. Geomembranes* 46, 1–10.
- Liu, S.H., Xue, X.H., Fan, K.W., Xu, S.Y., 2014. Earth pressure and deformation mode of a retaining wall constructed with soilbags. *Yantu Gongcheng Xuebao/Chinese J. Geotech. Eng.* 36, 2267–2273 (in Chinese).
- Matsuoka, H., Liu, S.H., 2005. A New Earth Reinforcement Method Using Soilbags. Taylor & Francis/Balkema, Netherlands.
- Naeini, S.A., Gholampoor, N., 2014. Cyclic behaviour of dry silty sand reinforced with a geotextile. *Geotext. Geomembranes* 42, 611–619.
- Qiang, N.D., Chai, J.C., 2015. Permeability of lime-and cement-treated clayey soils. *Can. Geotech. J.* 52, 1221–1227.
- Rowe, R.K., Skinner, G.D., 2001. Numerical analysis of geosynthetic reinforced retaining wall constructed on a layered soil foundation. *Geotext. Geomembranes* 19, 387–412.
- Sadrekarami, J., Abbasnejad, A., 2010. Arching effect in fine sand due to base yielding. *Can. Geotech. J.* 47, 366–374.
- Santos, E.C.G., Palmeira, E.M., Bathurst, R.J., 2013. Behaviour of a geogrid reinforced wall built with recycled construction and demolition waste backfill on a collapsible foundation. *Geotext. Geomembranes* 39, 9–19.
- Santos, E.C.G., Palmeira, E.M., Bathurst, R.J., 2014. Performance of two geosynthetic reinforced walls with recycled construction waste backfill and constructed on collapsible ground. *Geosynth. Int.* 21, 256–269.
- Shi, W., Chen, Q., Nimbalkar, S., Liu, W., 2017. A new mixing technique for solidifier and dredged fill in coastal area. *Mar. Georesour. Geotechnol.* 35, 52–61.
- Skinner, G.D., Rowe, R.K., 2005. Design and behaviour of a geosynthetic reinforced retaining wall and bridge abutment on a yielding foundation. *Geotext. Geomembranes* 23, 234–260.
- Song, F., Liu, H.B., Ma, L.Q., Hu, H.B., 2018. Numerical analysis of geocell-reinforced retaining wall failure modes. *Geotext. Geomembranes* 46, 284–296.
- Tang, Y., Miyazaki, Y., Tsuchida, T., 2001. Practices of reused dredgings by cement treatment. *Soils Found.* 41, 129–143.
- Tantono, S.F., Bauer, E., 2008. Numerical simulation of a soilbag under vertical compression. In: *Proc. 12th Int. Conf. Int. Assoc. Comput. Methods Adv. Geomech.*
- Tremblay, H., Duchesne, J., Locat, J., Leroueil, S., 2002. Influence of the nature of organic compounds on fine soil stabilization with cement. *Can. Geotech. J.* 39, 535–546.
- Wang, S., Luna, R., 2012. Monotonic behavior of Mississippi River Valley silt in triaxial compression. *J. Geotech. Geoenviron. Eng.* 138, 516–525.
- Xue, J.F., Chen, J.F., Liu, J.X., Shi, Z.M., 2014. Instability of a geogrid reinforced soil wall on thick soft Shanghai clay with prefabricated vertical drains: a case study. *Geotext. Geomembranes* 42, 302–311.
- Yang, G., Zhang, B., Lv, P., Zhou, Q., 2009. Behaviour of geogrid reinforced soil retaining wall with concrete-rigid facing. *Geotext. Geomembranes* 27, 350–356.
- Yoo, C., 2017. Serviceability state deformation behaviour of two-tiered geosynthetic reinforced soil walls. *Geosynth. Int.* 12–25.
- Zhang, J., Han, P., 2012. Displacement-based aseismic design method for gravity retaining walls large scale shaking table tests. *Chin. J. Geotech. Eng.* 34, 416–423 (in Chinese).
- Zhu, W., Zhang, C.L., Chiu, A.C.F., 2007. Soil–water transfer mechanism for solidified dredged materials. *J. Geotech. Geoenviron. Eng.* 133, 588–598.
- Zou, C., Wang, Y., Lin, J., Chen, Y., 2016. Creep behaviors and constitutive model for high density polyethylene geogrid and its application to reinforced soil retaining wall on soft soil foundation. *Construct. Build. Mater.* 114, 763–771.